OAK RIDGE NATIONAL LABORATORY
operated by
UNION CARBIDE CORPORATION
NUCLEAR DIVISION
for the
U.S. ATOMIC ENERGY COMMISSION

ORNL - TM - 2574

COPY NO. - 80

DATE - April 28, 1969

Neutron Physics Division

DOSE RATES IN A SLAB PHANTOM FROM MONOENERGETIC GAMMA RAYS

H. C. Claiborne and D. K. Trubey

Abstract

Gamma-ray flux-to-dose conversion factors obtained with a philosophy consistent with that used for neutron conversion factors have not been available for use in design work. To eliminate this inconsistency and develop more realistic gamma-ray conversion factors, gamma-ray dose rate distributions were determined in a slab phantom of a standard man composition.

Calculations were made with the discrete ordinates code ANISN with some checks by the Monte Carlo code OGRE. Based on these results, a recommended curve to convert gamma-ray flux to maximum dose rate delivered to a body was prepared for design use.

It is also recommended that a new unit, the maximum exposure dose (MED) be used in shield design work to express the product of the flux, dose-rate conversion factor, and quality factor for both gamma rays and neutrons.

NOTE:
This Work Partially Funded by
DEFENSE ATOMIC SUPPORT AGENCY
Under Subtask No. RRP-5033

INTRODUCTION

The response function or flux-to-dose conversion factor used for converting a calculated neutron flux to a dose rate is the maxiumum dose rate in the dose-rate distribution calculated by Snyder and Neufeld[1] for a unit flux (or current) of monoenergetic neutrons that are incident normally on a phantom represented by a slab of tissue. This is the conversion factor that is stipulated for use by the Federal Register[2] and generally has the force of law for reactor design. However, the Federal Register and the ICRP Committees[3,4] do not make adequate recommendation regarding response functions for gamma rays, and no calculations in tissue phantoms have been available previously for use in reactor or shelter design. (Alsmiller and Moran[5] obtained an approximate value for 10-MeV photons incident on a slab tissue phantom but their work was primarily for much higher incident photon energies.)

The ICRP Committees ignore the problem and the Federal Register merely states, "For determining exposures to X or gamma rays up to 3 MeV, the dose limits ... may be assumed to be equivalent to the 'air dose.' For the purpose of this part 'air dose' means that the dose is measured in a properly calibrated appropriate instrument in air at or near the body surface in the region of highest dose rate." Note that for gamma rays with energies > 3 MeV, no response function is stipulated.

The result is that air kerma and sometimes the tissue kerma in a free field as calculated by Henderson[6] have been used in design work. It must be pointed out that using these kerma gives a smaller calculated dose than the maximum dose that could be delivered to a body since

backscattering is not considered. In addition, the practice is certainly inconsistent with that adopted for neutrons.

In order to eliminate this inconsistency and provide standard gamma-ray dose response functions for design use, dose rates were calculated for gamma rays of various energies incident on a 30-cm-thick slab with the composition of the "standard man."[7] In the following sections the method of calculations and the results are discussed briefly.

The maximum dose rate in the dose-rate distribution curve and the integral dose rate (dose-rate distribution integrated over the slab) as a function of incident photon energy are shown in both tabular and graphical form and comparisons are made between discrete ordinates and Monte Carlo calculations of these quantities.

Calculational Model and Method

The dose-rate distribution in a slab phantom was calculated with the discrete ordinates code ANISN[8] using a $S_{16}P_5$ approximation. Some check calculations were made with OGRE,[9] a Monte Carlo code. An updated OGRE library was the source of the cross sections used in both types of calculations.

The Monte Carlo calculation used point values of the cross sections obtained by interpolation from the library, but for the discrete ordinates calculations, which were energy groups or bands, the library values were weighted on the basis of a flat flux spectrum using the MUG code.[10] The group transfer coefficients were obtained by a double integration over the two energy groups involved in the photon transfer.

In the Monte Carlo calculation pair production was treated as an absorption, but the discrete ordinates calculation considered transport of the 0.5-MeV gamma rays created as the result of the pair-production reaction. The (γ,n) reactions and other potential spallation reactions were ignored since the energies considered were not high enough for such reactions to make a significant contribution.

The phantom was a 30-cm-thick slab with the composition of the "standard man" (see Table I), which includes the eleven elements of significance contained in bone and tissue of an average man. The average density was taken as 1 g/cc.

For the discrete ordinates calculations the slab was divided into 36 increments. Starting with the source side there were eight 0.25-cm increments followed by 28 1-cm increments. The dose rates represented the average for the increment, which may be taken as the midpoint value.

Two group structures were used in order to reduce the calculation time and still maintain a sufficient fineness of energy structure. The number of groups and either the "high energy" or the "low energy" group structure were selected (see Table II)depending on the source energy. For the highest source energy in either of the group structures, all 23 groups were included, but for the next lowest energy source only 22 groups were used, etc. Discrete ordinates calculations were made for two types of sources: a straight-in or 0° monodirectional flux (same as current) and a plane isotropic flux. The two types represent limiting cases for a slab opposite a distributed source in a symmetric configuration.

TABLE I. ELEMENTAL PERCENTAGES AND NUMBER DENSITIES CONTAINED IN A STANDARD MAN

Element	%	Number Density (atoms/g)
		x 10^{24}
H	10	0.05977
O	60	0.02259
C	24	0.01204
N	2.9	0.00125
Ca	1.2	0.177-3*
P	1.1	0.214-3
S	0.24	0.451-3
K	0.20	0.308-4
Na	0.20	0.524-4
Cl	0.20	0.340-4
Mg	0.03	0.743-5

*Read as 0.177 x 10^{-3}.

For the Monte Carlo calculations in the slab, a total of 21 plane detectors was used. Starting at the source side, eleven plane detectors 1 cm apart followed by ten more 2 cm apart were assumed present. In all the calculations 2000 case histories were used with no importance sampling but with statistical estimation of the energy absorption. Only the straight-in monodirectional source condition was calculated with the Monte Carlo code.

Results and Discussion

The maximum gamma-ray dose rates in the dose-rate distributions that were calculated for the slab phantom as a function of incident photon energy are shown in Table II along with the calculated kerma for the "standard man" composition and the tissue kerma calculated by Henderson.[6] In all cases these maxima occurred within the first 2 cm except for the OGRE result for the 0.5-MeV source, which occurred at 2.5 cm. Note that the high- and low-energy structures overlap; the low-energy structure covers the energy range of group 15 through 23 of the high-energy structure. This arrangement was used as a compromise between maintaining a large number of groups for each source energy and reducing the amount of calculational effort as well as getting an indication of the effect of group structure. Figure 1 is effectively a plot of the results in Table II. The discrete ordinates curve is drawn through the higher of the dose rates obtained for the two source types (for all practical purposes, the normally incident flux) using the first 14 groups of the high-energy structure and all 23 groups of the low-energy structure. In plotting the ANISN results the incident

TABLE II. MAXIMUM GAMMA-RAY DOSE RATES IN THE DOSE-RATE DISTRIBUTION IN A SLAB PHANTOM[a]

Group No.	Group Energy Range, MeV	Dose Rates[b] for Normally Incident Flux (rads/hr)/(γ/cm²sec) ANISN	Dose Rates[b] for Normally Incident Flux (rads/hr)/(γ/cm²sec) OGRE	ANISN Dose Rates[c] for Isotropically Incident Flux (rads/hr)/(γ/cm²sec)	Kerma Rate[g] (rads/hr)/(γ/cm²sec) OGRE Lib.	Kerma Rate[g] (rads/hr)/(γ/cm²sec) Henderson[6]
High-Energy Structure:						
1	14-16	1.326-5[d]	1.317-5(0.029)[f]	1.331-5	1.311-5	
2	12-14	1.171-5		1.178-5	1.166-5	
3	10-12	1.021-5	9.458-6(0.037)[e]	1.024-5	1.017-5	
4	8-10	8.734-6		8.760-6	8.677-6	8.7-6
5	7-8	7.625-6		7.660-6	7.561-6	7.5-6
6	6.5-7	7.074-6		7.112-6	6.994-6	6.9-6
7	6.0-6.5	6.710-6		6.750-6	6.619-6	6.5-6
8	5.5-6.0	6.339-6		6.379-6	6.243-6	6.2-6
9	5.0-5.5	5.961-6	5.938-6(0.34)	6.003-6	5.865-6	5.8-6
10	4.5-5.0	5.579-6		5.620-6	5.481-6	5.4-6
11	4.0-4.5	5.190-6		5.230-6	5.055-6	5.0-6
12	3.5-4.0	4.785-6		4.822-6	4.664-6	4.5-6
13	3.0-3.5	4.365-6		4.398-6	4.216-6	4.1-6
14	2.6-3.0	3.969-6		3.996-6	3.800-6	3.70-6
15	2.2-2.6	3.596-6		3.616-6	3.424-6	3.35-6
16	1.8-2.2	3.200-6	3.143-6(0.42)	3.210-6	3.012-6	2.76-6
17	1.35-1.8	2.727-6		2.721-6	2.522-6	2.47-6

TABLE II (cont.)

Group No.	Group Energy Range, MeV	Dose Rates[b] for Normally Incident Flux (rads/hr)/(γ/cm^{2}sec) ANISN	OGRE	ANISN Dose Rates[c] for Isotropically Incident Flux (rads/hr)/(γ/cm^{2}sec)	Kerma Rate[g] (rads/hr)/(γ/cm^{2}sec) OGRE Lib.	Henderson[6]
18	0.9-1.35	2.141-6		2.109-6	1.955-6	1.86-6
19	0.6-0.9	1.581-6		1.516-6	1.383-6	1.30-6
20	0.4-0.6	1.173-6	1.140-6(1.5)	1.077-6	9.432-7	9.27-7
21	0.2-0.4	7.208-7	7.363-7(1.9)	6.088-7	5.471-7	5.50-7
22	0.1-0.2	4.506-7			2.393-7	2.37-7
23	0.1-0.01				1.332-7	1.31-7
Low Energy Structure:						
1	2.48-2.72	3.789-6		3.815-6	3.626-6	
2	1.92-2.48	3.399-6		3.418-6	3.215-6	
3	1.68-1.92	2.999-6		3.003-6	2.783-6	
4	1.12-1.68	2.505-6		2.494-6	2.306-6	
5	0.88-1.12	1.995-6		1.961-6	1.776-6	1.76-6
6	0.72-0.88	1.692-6		1.643-6	1.468-6	1.44-6
7	0.68-0.72	1.534-6	1.500-6(1.1)	1.478-6	1.297-6	1.26-6
8	0.62-0.68	1.445-6		1.385-6	1.216-6	1.17-6
9	0.58-0.62	1.357-6		1.292-6	1.127-6	1.10-6
10	0.52-0.58	1.264-6		1.196-6	1.034-6	1.01-6
11	0.48-0.52	1.173-6	1.140-6(1.5)	1.102-6	9.432-7	9.27-7

TABLE II (cont.)

Group No.	Group Energy Range, MeV	Dose Rates[b] for Normally Incident Flux (rads/hr)/(γ/cm²sec) ANISN	OGRE	ANISN Dose Rates[c] for Isotropically Incident Flux (rads/hr)/(γ/cm²sec)	Kerma Rate[g] (rads/hr)/(γ/cm²sec) OGRE Lib.	Henderson[6]
12	0.42-0.48	1.074-6		9.991-7	8.454-7	8.16-7
13	0.38-0.42	9.769-7		8.991-7	7.497-7	7.39-7
14	0.32-0.38	8.663-7		7.859-7	6.469-7	6.44-7
15	0.28-0.32	7.565-7	7.363-7(1.9)	6.762-7	5.471-7	5.50-7
16	0.22-0.28	6.196-7		5.371-7	4.414-7	4.44-7
17	0.18-0.22	5.185-7		4.367-7	3.408-7	3.38-7
18	0.12-0.18	3.826-7		3.026-7	2.393-7	2.37-7
19	0.08-0.12	2.765-7		1.989-7	1.509-7	1.49-7
20	0.06-0.08	2.661-7		2.019-7	1.244-7	1.24-7
21	0.04-0.06	2.821-7			1.431-7	1.40-7
22	0.02-0.04	5.867-7			3.407-7	3.34-7
23	0.01-0.02				1.462-7	1.40-7

[a] Infinite slab 30-cm thick; 11-element standard man[7] composition; density, 1 g/cc.

[b] Normalized to one photon/cm²sec crossing the surface.

[c] Normalized to a flux of unity in the forward hemisphere or 1/2 photon/cm sec crossing the surface.

[d] Read as 1.326×10^{-5}.

[e] Monte Carlo result for 10-MeV gamma ray.

[f] Parentheses include the estimated standard deviation in %.

[g] In the Monte Carlo and the kerma calculations, monoenergetic sources at the group mid-point energy were used.

ORNL-DWG-69-4602

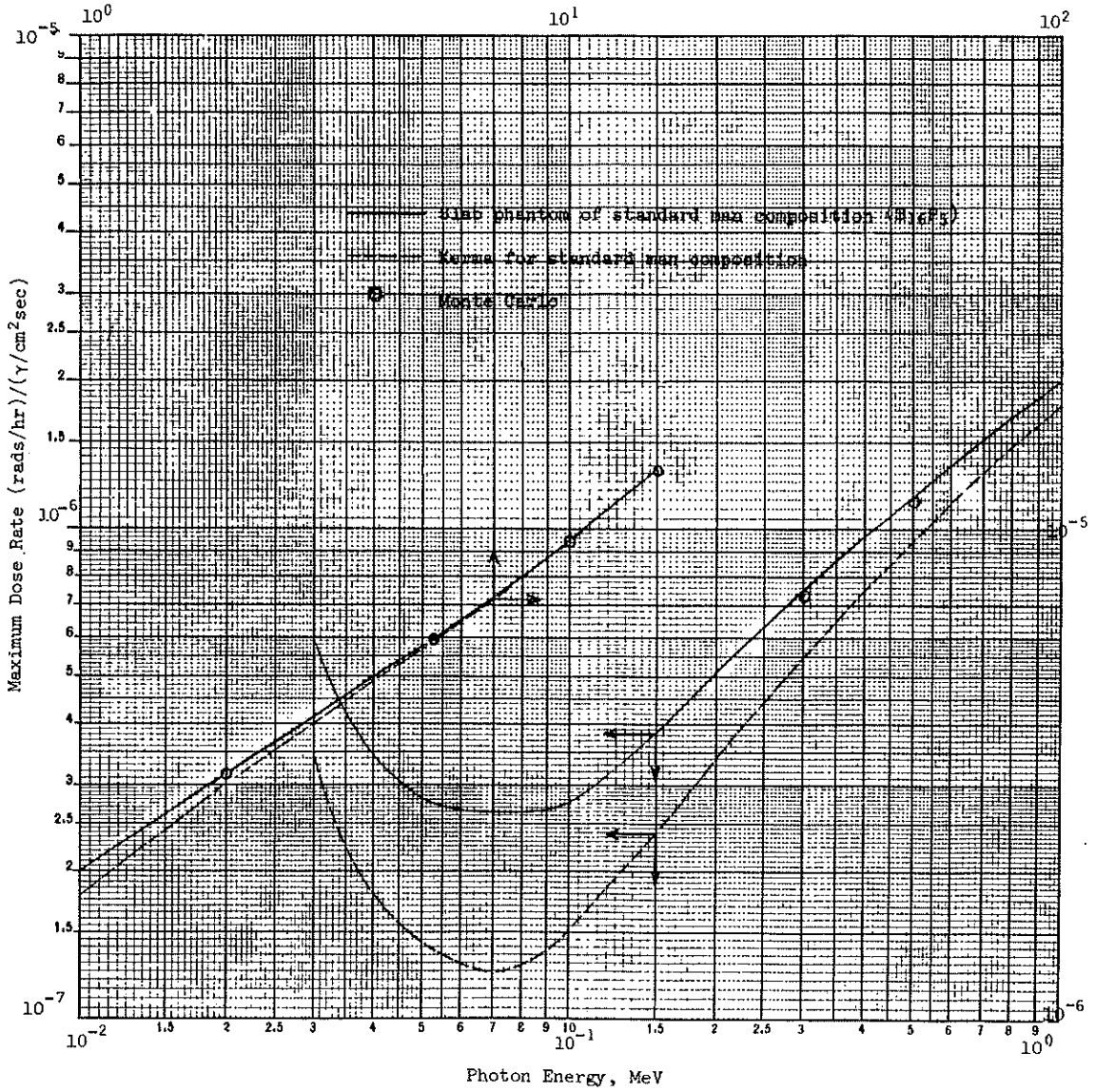

Fig. 1. Gamma-Ray Flux to Dose Rate Conversion Factors

photon energy was taken as equal to the midpoint value of the group range. More properly a bar graph should be shown, but this is of no significance in practical applications.

Table III shows the total or integral dose rate obtained by integrating the dose-rate distribution over the slab thickness. Figure 2 is a plot of these results using the first 14 source groups of the high-energy structure and all source groups of the low-energy structure. The average value is obtained by dividing by the slab thickness, 30 cm. Note that unlike the maximum dose rate, the integrated dose is quite different for the two source types. Both are normalized to a unit incident flux in the forward hemisphere but in the isotropic case the current is only half the value of the straight-in case, for which flux and current are equal. As the source energy decreases and the slab penetration decreases the ratio of the straight-in to the isotropic dose approaches 2, which implies that the effect of backscattering from the slab is small.

Figure 3 shows plots of dose-rate distributions for three representative source energies. Peaking of the dose-distribution curve was not apparent for source energies greater than 2 MeV. With smaller source energies the maximum dose rate occurred at increasing depths until a maximum of 2 cm was reached for the 0.08-0.12 MeV source; for still smaller energies the peak depth decreased.

As Table II shows, all the estimated statistical deviations were within 2% for the Monte Carlo calculation of the maximum dose rate. The uncertainty is small since there is no statistical error associated with the uncollided flux which is dominant at this position. The

ORNL-DWG-69-4603

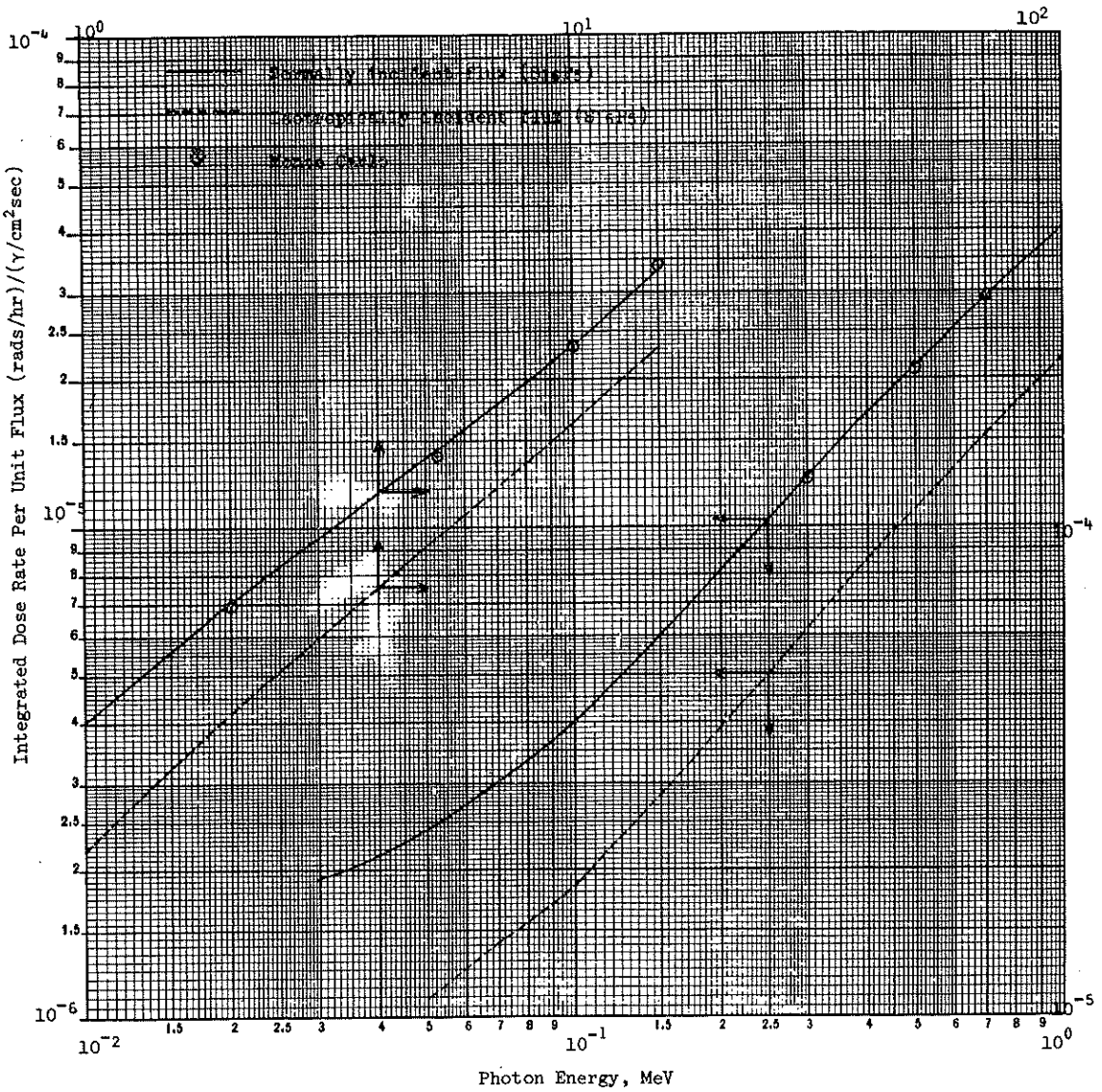

Fig. 2. Gamma-Ray Dose Rates Integrated Over the Thickness of the Slab Phantom

TABLE III. INTEGRAL DOSE RATES IN A SLAB PHANTOM[a]

Group No.	Group Energy Range, MeV	Dose Rates[b] for Normally Incident Flux (cm rads/hr)/(γ/cm²sec) ANISN	Dose Rates[b] for Normally Incident Flux (cm rads/hr)/(γ/cm²sec) OGRE	ANISN Dose Rates[c] for Isotropically Incident Flux (cm rads/hr)/(γ/cm²sec)
High Energy Structure:				
1	14-16	3.308-4[d]	3.400-4	2.325-4
2	12-14	2.920-4		2.042-4
3	10-12	2.542-4	2.329-4[e]	1.764-4
4	8-10	2.164-4		1.485-4
5	7-8	1.877-4		1.274-4
6	6.5-7	1.733-4		1.167-4
7	6.0-6.5	1.637-4		1.096-4
8	5.5-6.0	1.539-4		1.023-4
9	5.0-5.5	1.439-4	1.394-4	9.496-5
10	4.5-5.0	1.337-4		8.747-5
11	4.0-4.5	1.233-4		7.982-5
12	3.5-4.0	1.125-4		7.195-5
13	3.0-3.5	1.013-4		6.384-5
14	2.6-3.0	9.077-5		5.627-5
15	2.2-2.6	8.088-5		4.928-5
16	1.8-2.2	7.040-5	6.935-5	4.199-5
17	1.35-1.8	5.825-5		3.379-5
18	0.9-1.35	4.387-5		2.449-5
19	0.6-0.9	3.060-5		1.635-5
20	0.4-0.6	2.107-5	2.098-5	1.078-5
21	0.2-0.4	1.256-5		6.149-6
22	0.1-0.2	6.450-6		
23	0.1-0.01			
Low Energy Structure:				
1	2.48-2.72	8.604-5		5.293-5
2	1.92-2.48	7.583-5		4.576-5
3	1.68-1.92	6.510-5		3.836-5

TABLE III (cont)

Group No.	Group Energy Range, MeV	Dose Rates[b] for Normally Incident Flux (cm rads/hr)/(γ/cm^{2}sec) ANISN	OGRE	ANISN Dose Rates[c] for Isotropically Incident Flux (cm rads/hr)/(γ/cm^{2}sec)
4	1.12-1.68	5.300-5		3.036-5
5	0.88-1.12	4.017-5		2.210-5
6	0.72-0.88	3.300-5		1.772-5
7	0.68-0.72	2.926-5	2.916-5	1.548-5
8	0.62-0.68	2.531-5		1.434-5
9	0.58-0.62	2.331-5		1.319-5
10	0.52-0.58	2.128-5		1.205-5
11	0.48-0.52	2.128-5	2.098-5	1.090-5
12	0.42-0.48	1.919-5		9.744-6
13	0.38-0.42	1.708-5		8.585-6
14	0.32-0.38	1.489-5		7.405-6
15	0.28-0.32	1.267-5	1.251-5	6.224-6
16	0.22-0.28	1.031-5		5.016-6
17	0.18-0.22	8.191-6		3.932-6
18	0.12-0.18	6.028-6		2.838-6
19	0.08-0.12	3.996-6		1.852-6
20	0.06-0.08	3.064-6		1.425-6
21	0.04-0.06	2.321-6		1.091-6
22	0.02-0.04	1.592-6		
23	0.01-0.02			

[a] Dose-rate distribution integrated over 30-cm-thick slab; 11-element standard man[7] composition.

[b] Normalized to one photon/cm^{2}sec crossing the surface.

[c] Normalized to a flux of unity in the forward hemisphere or 1/2 photon/cm^{2}sec crossing the surface.

[d] Read as 1.326×10^{-5}.

[e] Monte Carlo result for 10-MeV gamma ray.

[f] Parentheses include the estimated standard deviation in %.

[g] In the Monte Carlo and the tissue kerma calculations, monoenergetic sources at the group mid-point energy were used.

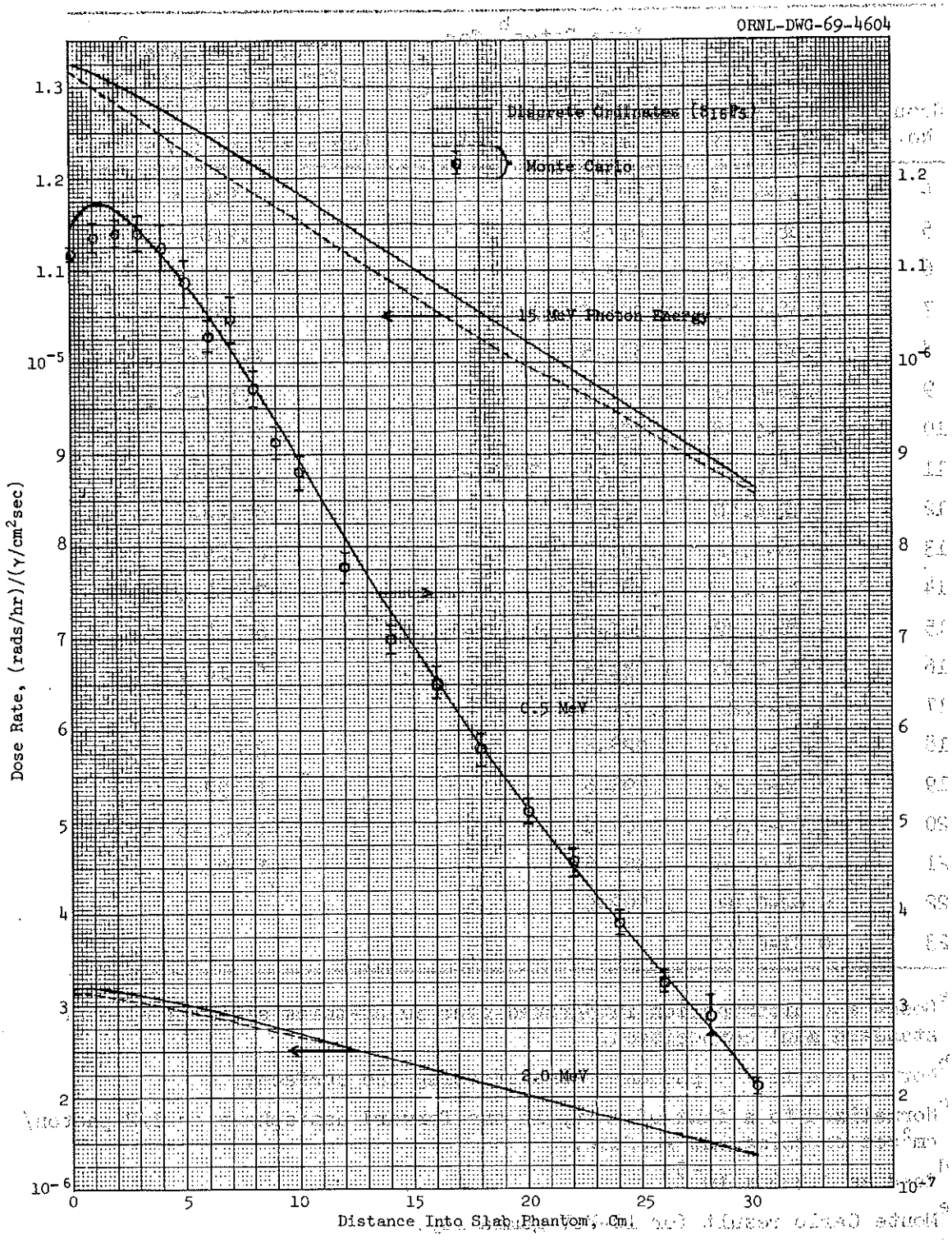

Fig. 3. Dose Rate Distribution in Slab Phantom For Normally Incident Gamma Rays.

statistics for deeper penetration were not as good, particularly for the lower energies. This is shown in Figure 3 by the "error bars" for the 0.5-MeV source. It was for the penultimate detector of this calculation that the largest estimated standard deviation (7.5%) occurred.

Conclusions

It may be generally concluded after a detailed study of the tables and figures that:

1. The good agreement between the discrete ordinates and the Monte Carlo results indicate that truncation errors, the effect of monoenergetic or band sources and the effect of transport of the 0.5-MeV annihilation gamma rays are small.
2. The effect of group structure is small providing that the structure is not too coarse at the lower energies.
3. The difference in the maximum dose rate as a result of a normally incident flux or an isotropically incident flux (when normalized to equal fluxes in the forward hemisphere) is not significant except at the lower energies.
4. The differences between the maximum dose rates in a slab phantom and kerma in a free field are insignificant above about 2 MeV but as the incident photon energy decreases the difference increases at 0.07 MeV.
5. Comparison with Henderson's[5] tissue kerma shows the "standard man" kerma are higher by at most a few percent. Most of this undoubtedly results from the atoms of higher atomic numbers that are not present in the Henderson[5] four-element tissue model.

Recommendations

We recommend that the maximum dose rates for the slab phantom as shown in Figure 3 be used as a standard gamma-ray response function in design work. We further recommend that this calculated dose rate (as well as similar phantom dose rates for neutrons) be called the maximum exposure dose (MED) when multiplied by the Quality Factor.

REFERENCES

1. W. S. Snyder and C. Neufeld, "On the Passage of Heavy Particles Through Tissue," Radiation Res. 6, 67 (1957). Also in NBS Handbook 63.

2. Federal Register, Title 10, Part 20, "Standards for Protection Against Radiation" (1966).

3. Recommendations of the International Commission on Radiological Protection. Report of Committee III, Protection Against X-Rays up to Energies of 3 MeV and Beta and Gamma Rays from Sealed Sources. ICRP Publication 3. Pergammon Press, New York (1960).

4. Recommendations of the International Commission on Radiological Protection. Report of Committee IV. Protection Against Electromagnetic Radiation Above 3 MeV and Electrons, Neutrons, and Protons. Pergammon Press, New York (1964).

5. R. G. Alsmiller, Jr., and H. S. Moran, "Dose Rate From High-Energy Electrons and Photons," Nucl. Instr. and Methods 58, 343 (1968).

6. B. J. Henderson, "Conversion of Neutron or Gamma-Ray Flux to Absorbed Dose Rate," XDC 59-8-179, General Electric Co. (1959).

7. J. J. Ritts, E. Solomito, and P. N. Stevens, "Calculations of Neutron Fluence-to-Kerma Factors for the Human Body," ORNL-TM-2079, Oak Ridge National Laboratory (1968).

8. W. W. Engle, Jr., "A User's Manual for ANISN, A One-Dimensional Discrete Ordinates Transport Code with Anisotropic Scattering," K-1693, Union Carbide Corporation, Nuclear Division (1967).

9. S. K. Penny, D. K. Trubey, M. B. Emmett, "OGRE, A Monte Carlo System for Gamma-Ray Transport Studies, Including an Example (OGRE-P1) for Transmissions Through Laminated Slabs," ORNL-3805, Oak Ridge National Laboratory (1966).

10. J. R. Knight, "MUG." Unpublished FORTRAN program of the Computing Technology Center, Union Carbide Corporation, Nuclear Division.

DASA SHIELDING DISTRIBUTION

Director, Advanced Research Projects Agency, Washington, D. C. 20301

Commanding Officer, Armed Forces Radiobiology Research Institute, National Naval Medical Center, ATTN: Technical Library: Mr. C. W. Garrett, Bethesda, Maryland 20014 (2 copies)

Director, Defense Atomic Support Agency, ATTN: APTL; Mr. Haas, DDST (For TTCP-N4), Washington, D. C. 20305 (17 copies)

Director, Defense Communications Agency, ATTN: NMCSSC, B-210, Washington, D. C. 20305

Defense Documentation Center, Cameron Station, Alexandria, Virginia 22314 (20 copies)

Director, Defense Intelligence Agency, ATTN: DIAAP-SB, Washington, D. C. 20301

Office of Defense Research and Engineering, Assistant Director (Nuclear Programs), Room 3E1071, The Pentagon, ATTN: Technical Library; Asst Dir (Strategic Weapons); Asst Dir (Command & Control), Washington, D. C. 20301 (3 copies)

Joint Chiefs of Staff, Department of Defense, ATTN: Technical Library, Washington, D. C. 20301

Commander, Joint Task Force Eight, ATTN: Technical Library, Sandia Base, New Mexico 87115

Chief, National Military Command System Support Center, Room BE-685, The Pentagon, ATTN: Technical Library, Washington, D. C. 20301

Director, Weapons Systems Evaluation Group, ATTN: Library/Col Holden/C. Beckels, Washington, D. C. 20305

Joint Strategic Target Planning Staff, Offutt AFB, Nebraska 68113
ATTN: JLTW, LTC Maloney

Commanding Officer, U. S. Army Combat Developments Command, Institute of Nuclear Studies, Fort Bliss, Texas 79916

Chief of Research and Development, Department of the Army, ATTN: Nuclear, Chemical-Biological Division, Washington, D. C. 20310

Commanding General, U. S. Army Electronics Proving Ground, ATTN: Technical Library, Fort Huachuca, Arizona 85613

Chief of Engineers, Department of the Army, ATTN: ENGMC-EM, Washington, D. C. 20315

Commanding Officer, U. S. Army Mobility Equipment Research & Development Center, ATTN: Technical Info & Library Branch, Fort Belvoir, Virginia 22060

Director, U. S. Army Engineer Waterways Experiment Station, ATTN: Library, Vicksburg, Mississippi 39180

Commanding Officer, Harry Diamond Laboratories, ATTN: Technical Reference Branch, Washington, D. C. 20438

Commanding General, U. S. Army Materiel Command, ATTN: AMCRD-BN/Nuclear Branch, Washington, D. C. 20315

U. S. Army Sentinel Systems Command, Redstone Arsenal, ATTN: Technical Library, Huntsville, Alabama 35809

Commanding Officer, U. S. Army Nuclear Defense Laboratory, ATTN: Library, Edgewood Arsenal, Maryland 21010

Surgeon-General, Department of the Army, Room 1616, Main Navy Bldg., Washington, D. C. 20315

Commanding General, White Sands Missile Range, ATTN: Technical Library/ ORDBS-OM-TL, Las Cruces, New Mexico 88002

Commanding Officer, Picatinny Arsenal, Dover, New Jersey 07801

Commanding Officer, U. S. Army Research Office (Durham), Box CM, Duke Station, ATTN: Technical Library, Durham, North Carolina 27706

Commanding General, U. S. Army Tank-Automotive Center, Warren, Michigan 48090

Commanding General, U. S. Army Test and Evaluation Command, ATTN: NBS Office, Aberdeen Proving Ground, Maryland 21005

Office of the Secretary of the Army, Director of Civil Defense, ATTN: Research, Washington, D. C. 20310

Commanding General, Frankfort Arsenal, Bridge and Tacony Streets, Philadelphia, Pennsylvania 19137

Commanding Officer, U. S. Army Materials Research Agency, ATTN: Technical Library Section, Watertown Arsenal, Watertown, Massachusetts 02172

Commanding Officer, Naval Civil Engineering Laboratory, Port Huenema, California 93041

Chief of Naval Operations, Department of the Navy, ATTN: OP 75, Washington, D. C. 20350

Superintendent, Naval Postgraduate School, ATTN: Technical Library, Monterey, California 93940

Commanding Officer, Naval Radiological Defense Laboratory, ATTN: Tech Info Div., Dr. J. Ferguson, San Francisco, California 94135 (2 copies)

Director, Naval Research Laboratory, ATTN: Technical Library, Washington, D. C. 20390

Commander, Naval Ship Systems Command, Department of the Navy, ATTN: L. E. Seiffert, CODE 03541, Washington, D. C. 20360

Commanding Officer, Nuclear Weapons Training Center Atlantic, ATTN: Technical Library, Norfolk, Virginia 23511

Commander, Air Defense Command, ATTN: ADLMD-W, Missile & Space Weapon Div.; ADLDC, DCS/Plans; ADCSG, Box 35 (Col Kossuth), Ent Air Force Base, Colorado 80912 (3 copies)

Dirctor, Air University Library, Maxwell AFB, Alabama 36112

Arnold Engineering Development Center, ATTN: AELR, Arnold AFB, Tennessee 37389

ATC, ATTN: Office of the Surgeon, Randolph AFB, Texas 78148

Air Force Avionics Laboratory, ATTN: AVPT, Wright-Patterson AFB, Ohio 45433

Space & Missile System s Organization (SAMSO), AF Unit Post Office, ATTN: SMQN; SMTSM-1; SMSDM/STINFO/Technical Library, SMTSS, Los Angeles, California 90045 (4 copies)

Directorate of Nuclear Safety, ATTN: AFINS, Kirtland AFB, New Mexico 87117

Air Force Materials Laboratory, ATTN: MAS (Maj H. S. Reinert), Wright-Patterson AFB, Ohio 45433

Medical Service School/114, ATTN: MSSMDM, Sheppard AFB, Texas 76311

AF Office of Aerospace Research, Office of Research Analysis, ATTN: RRRD, Holloman AFB, New Mexico 88330

Commander, AF Office of Aerospace Research, 1400 Wilson Blvd., ATTN: RROSP, Arlington, Virginia 22209

Commander, USAF RADL Health Laboratory, ATTN: SGHW, Wright-Patterson AFB, Ohio 45433

Commander, Rome Air Development Center, ATTN: EMTLD (Documents Library), Griffis AFB, New York 13440

School of Aviation Medicine, USAFSC Aerospace Med Ctr, ATTN: Chief Radiobiology Branch, Brooks AFB, Texas 78235

AF Strategic Air Command, ATTN: OAI:DPLBIC (LTC Tye), Offutt AFB, Nebraska 68113

Air Force Systems Command, ATTN: SCS-7; SCTSW, Andrews AFB, Washington, D. C. 20331 (2 copies)

AFSC STLO, Air Force Unit Post Office, ATTN: TRSAL, Los Angeles, California 90045

ASD (ASNNS), WPAFB-OH 45433, ATTN: ASNNS, Wright-Patterson AFB, Ohio

Headquarters, USAF, ATTN: AFSCAMI-2; AFOCC-A; AFRDQSN; AFRDDF; AFRDD; AFOCE-KA, Washington, D. C. 20330 (6 copies)

Hq USAF, TEMPO-8, ATTN: AFMSR; AFTAC/SDP-R, Washington, D. C. 20333 (2 copies)

AF Weapons Laboratory, ATTN: WLRP; WLRB; WLDC; WLDN; WLIL; WLPM, Kirtland AFB, New Mexico 87117 (6 copies)

Argonne National Laboratory, 9700 South Cass Avenue, ATTN: Library Services Dept/Report Section, Argonne, Illinois 60440

U. S. Atomic Energy Commission, ATTN: Headquarters Library, Reports Section, Mail Station G-17, Washington, D. C. 20545

U. S. Atomic Energy Commission, Div. of Technical Information Extension, P. O. Box 62, Oak Ridge, Tennessee 37831

Brookhaven National Laboratory, ATTN: Research Library, Upton, New York 11973

University of California, Lawrence Radiation Laboratory, P. O. Box 808, ATTN: Technical Library, Livermore, California 94551

Los Alamos Scientific Laboratory, P. O. Box 1663, ATTN: R. F. Taschek/J. A. Phillips/G. A. Sawyer/E. J. Stovall, Los Alamos, New Mexico 87544 (4 copies)

Sandia Corporation, P. O. Box 5800, ATTN: Document Library, Albuquerque, New Mexico 87115

National Bureau of Standards, Radiation Theory Section, ATTN: Mr. G. M. Eisenhauer, Washington, D. C. 20239

National Center for Atmospheric Research, ATTN: Tech Library, Boulder, Colorado 80302

Public Health Service, 4th and Jefferson Drive, S.W., ATTN: Mr. C. L. Weaver, Washington, D. C. 20201

USPHS, Research Branch, Division of Radiological Health, 1901 Chapman Ave., Rockville, Maryland 20853

Mr. Gilbert J. Ferber and Dr. L. Machta, Air Resources Laboratory, ESSA, Georgia Avenue, Silver Spring, Maryland

Aerojet-General Corp., San Ramon Plant, P. O. Box 86, San Ramon, California 94583 ATTN: Technical Library

Aerospace Corp., 1111 E. Jill Street, ATTN: Dr. E. W. Ray; Dr. Benveniste, San Bernardino, California 92402 (2 copies)

Battelle Memorial Institute, 505 King Avenue, Columbus, Ohio 43201 ATTN: Mr. John E. Davis

Battelle Memorial Institute, Pacific Northwest Laboratory, P. O. Box 999, Richland, Washington 99352

Philco-Ford Corporation, Aeronutronic Division, Ford and Jamborree Roads, ATTN: Technical Library, Newport Beach, California

The Bendix Corporation Missile Systems Division, 400 South Beiger Street, ATTN: Technical Library, Mishawaka, Indiana 46544

Boeing Aircraft Company, P. O. Box 3707, ATTN: Technical Library, Seattle, Washington 98108

Columbia University, Low Memorial Library, ATTN: Dr. H. Goldstein Physics Department, New York, New York 10027

Gulf General Atomic, P. O. Box 608, San Diego, California 92112 ATTN: Dr. J. R. Beyster

General Dynamic/Convair (Astronautics), 5001 Kearny Villa Road, P. O. Box 1128, ATTN: Technical Library/Dr. D. Hamlin, San Diego, California 92112

General Dynamics Corporation, Fort Worth Division, P. O. Box 748, ATTN: Technical Library, Fort Worth, Texas 76101

General Electric Company, TEMPO, Center for Advanced Studies, 816 State Street, ATTN: DASA Information and Analysis Center/W. W. Chan, Santa Barbara, California 93102

Holmes and Narver, Inc., 828 S. Figueroa Street, ATTN: Nuclear Division Library, Los Angeles, California 90017

IIT Research Institute, 10 West 35th Street, Chicago, Illinois 60616 ATTN: Technical Library

University of Illinois, Urbana Campus, ATTN: Dr. A. B. Chilton, Urbana, Illinois 61801

Institute for Defense Analyses, 400 Army-Navy Drive, ATTN: Technical Information Office, Arlington, Virginia 22202

Kaman Corporation, Kaman Nuclear Division, Garden of the Gods Road, Colorado Springs, Colorado 80907

Knolls Atomic Power Laboratory, P. O. Box 1072, ATTN: Document Library, Schenectady, New York 12301

Massachusetts Institute of Technology, Instrumentation Laboratory, 68 Albany Street, ATTN: Technical Library, Cambridge, Massachusetts

Lockheed Missiles and Space Company, 3251 Hanover Street, Palo Alto, California 94304

Martin-Marietta Corporation, P. O. Box 179, ATTN: Technical Library, Denver, Colorado 80291

Massachusetts Institute of Technology, 68 Albany Street, ATTN: MIT Libraries-Technical Reports, Cambridge, Massachusetts 02139

University of Michigan, P. O. Box 618, ATTN: Technical Library, Ann Arbor, Michigan 48107

North American Aviation, Space and Information Systems Division, 12214 Lakewood Blvd., Downey, California 90241 ATTN: Engineering Library

Northrop Corporate Laboratories, 3401 West Broadway, Hawthorne, California 90250 ATTN: Dr. D. A. Hicks

Radiation Research Associates, Inc., 3550 Hulen Street, Fort Worth, Texas 76107

The RAND Corporation, 1700 Main Street, ATTN: Dr. J. I. Marcum, Santa Monica, California 90406

Stanford Research Institute, ATTN: Technical Library, 333 Ravenswood Ave., Menlo Park, California 94025

Sylvania Electronic Products, 190 Whisman Avenue, Mountain View, California 94042

Technical Operations, Inc., South Avenue, Burlington, Massachusetts 01803

LFE, Inc., Tracerlab Division, 2030 Wright Avenue, Richmond, California 94808

TRW Systems One Space Park, ATTN: Miss Nancy Hammond, Librarian, Redondo Beach, California 90278

Union Carbide Corporation, Union Carbide Research Institute, P. O. Box 278, Tarrytown, New York 10592

United Nuclear Corporation, 5 New Street, White Plains, New York 10601

University of Virginia, ATTN: Nuclear Engineering Department-Dr. Reed Johnson, Charlottsville, Virginia 22901

National Academy of Sciences, 2101 Constitution Avenue, Washington, D. C. 20418

Space Technology Laboratories, 5771 West 96th Street, Bldg. 12, Los Angeles, California

TRW, RAMO-Woolridge Division, 8433 Fallbrook Avenue, ATTN: Technical Library, Canoga Park, California

Research Triangle Institute, P. O. Box 12194, Research Triangle Park, North Carolina 27709

Courant Institute of Mathematical Sciences, 251 Mercer Street, ATTN: Dr. M. H. Kalos, New York, New York 10012

Ottawa University, Department of Physics, ATTN: Dr. L. Spencer, Ottawa, Kansas 66067

Hughes Aircraft Company, ATTN: Doris Foehner, 3011 Malibu Canyon Road, Malibu, California 90265

University of Maryland, Department of Chemical Engineering, College Park, Maryland 20740

Kansas State University, Department of Nuclear Engineering, ATTN: Dr. W. Kimel, Manhattan, Kansas 66502

Associated Nucleonics, Inc., 975 Stewart Avenue, Garden City, New York 11552

Carnegie Institute of Technology, Department of Physics, Pittsburgh, Pennsylvania 15213

Marquardt Corp., 16555 Saticoy Street, Van Nuy, California 91406

Nuclear-Chicago Corp., 333 E. Howard Avenue, Des Plaines, Illinois 60018

Texas Nuclear Corp., Box 9267, Allendale Station, Austin, Texas 78756

University of California, Civilian Defense Research Project, 741 University Hall, 2200 University Avenue, Berkeley, California 94720

ORNL-TM-2574

INTERNAL DISTRIBUTION

1- 3. L. S. Abbott
4. R. G. Alsmiller, Jr.
5. E. D. Arnold
6. J. A. Auxier
7-56. H. C. Claiborne
57. C. E. Clifford
58. A. P. Fraas
59. F. C. Maienschein
60. J. P. Nichols
61. S. K. Penny
62. R. W. Roussin
63. L. B. Shappert
64. W. S. Snyder
65. E. Solomito
66. P. N. Stevens
67. E. A. Straker
68. D. K. Sundberg
69-73. D. K. Trubey
74. J. V. Wilson
75. E. R. Cohen (consultant)
76. B. C. Diven (consultant)
77. W. N. Hess (consultant)
78. M. H. Kalos (consultant)
79. L. V. Spencer (consultant)
80-81. Central Research Library
82. ORNL Y-12 Technical Library
83. Document Reference Section
84-85. Laboratory Records Dept.
86. Laboratory Records ORNL RC
87. ORNL Patent Office

EXTERNAL DISTRIBUTION

88-199. Given DASA Distribution as listed on the preceding pages.
200. Lt. Anthony R. Buhl, USA-Nuclear Defense Laboratory, Edgewood Arsenal, Maryland 21010
201. Prof. Herbert Goldstein, Room 287A, Mudd Building, Columbia University, New York, New York 10027
202. W. H. Hannum, Division of Reactor Development and Technology, U. S. Atomic Energy Commission, Washington, D. C.
203. P. B. Hemmig, Division of Reactor Development and Technology, U. S. Atomic Energy Commission, Washington, D. C.
204. E. A. Warman, Manager, Shielding Analysis, Nuclear Rocket Operations, Aerojet-General Corporation, Box 15847, Sacramento, California 95813
205-219. Division of Technical Information Extension (DTIE)
220. Laboratory and University Divison (ORO)
221. Kermit O. Laughon, AEC Site Representative